Diffraction and XPS Studies of Misfit Layer Chalcogenides Intercalated with Cobaltocene

L. Hernán, J. Morales, L. Sánchez, and J. L. Tirado

Laboratorio de Química Inorgánica, Facultad de Ciencias, Universidad de Córdoba, Avda. San Alberto Magno s/n, 14004 Córdoba, Spain

J. P. Espinós and A. R. González Elipe

Instituto de Ciencias de Materiales, Centro Mixto Universidad de Sevilla, CSIC, P.O. Box 1115, Seville, Spain

Received March 23, 1995. Revised Manuscript Received June 2, 1995[⊗]

Polycrystalline samples of $(PbS)_{1.18}(TiS_2)_2$, $(PbS)_{1.14}(TaS_2)_2$, and $(PbSe)_{1.12}(NbSe_2)_2$, ternary chalcogenides, have been intercalated with cobaltocene by direct reaction of the organometallic compound in acetonitrile solutions. Powder X-ray and electron diffraction data support a model in which the cobaltocene molecule is located in all TX_2-TX_2 (T = transition metal; X = S^{2-} or Se^{2-}) interfaces of these misfit layer compounds, whereas the $MX-TX_2$ (M = Pb) interfaces are empty. X-ray photoelectron spectroscopy (XPS) revealed the presence of two different oxidized cobalt species in these intercalated samples. Thus, in situ experiments of cobaltocene deposition from the gas phase, under UHV conditions, onto clean surfaces of binary and ternary chalcogenides, allowed the identification of these cobalt species as $CoCp_2$ and $[CoCp_2]^+$ (Cp = η^5-C_5H_5). It has also been shown by XPS that the intercalation of cobaltocene does not affect the core binding energies of the host matrix elements.

Introduction

The intercalation reaction of organometallic sandwich compounds, in particular cobaltocene, in transition-metal dichalcogenides, has been extensively investigated since the first report published by Dines.[1-8] Later, different authors have succeeded in the intercalation of this metallocene into tin dichalcogenides[9] and into different transition-metal phosphotrichalcogenides.[10,11]

More recently a new family of composite layered chalcogenides with $(MX)_{1+y}(TX_2)_2$ stoichiometry (M = Sn, Pb, Bi; T = Ti, Nb, Ta; X = S, Se) have been synthesized and characterized.[12] Until now, X-ray single-crystal structures have been determined only for $(PbS)_{1.14}(NbS_2)_2$,[13] $(PbS)_{1.18}(TiS_2)_2$,[14] and $(PbSe)_{1.12}(NbSe_2)_2$.[15] A common feature of these compounds is a misfit layer type structure consisting of a double layer MX and two TX_2 sandwiches stacked along the *c* axis. In fact, these compounds can be considered as stage II intercalation compounds of transition-metal dichalcogenides. The atomic arrangement of MX sublattice is similar to that of double layer in TlI and is based on a distorted NaCl structure. The TX_2 sandwich has an atomic arrangement identical to the TX_2 unit of the binary transition metal dichalcogenide. The two subcells have both the *b* axis in common, and the ratio of the lengths of the *a* axis is irrational.

From the point of view of intercalation reactions these compounds have an outstanding characteristic: the formation of van der Waals gaps between adjacent TX_2 slabs with vacant octahedral and tetrahedral interstitial positions available to different guest species. Thus, they are unique to constrast the behavior and properties of the same guest molecule intercalated in structurally related lattices such as transition-metal dichalcogenides. At present, alkali metals such as lithium and sodium,[16-19] and compounds such as hydrazine[20] have been successfully intercalated. In a recent preliminary report[21] a novel intercalation complex was obtained by

[⊗] Abstract published in *Advance ACS Abstracts,* July 1, 1995.

(1) Dines, M. B. *Science* **1975**, *188*, 1210.
(2) Sibernagel, B. G. *Chem. Phys. Lett.* **1975**, *34*, 298.
(3) Davies, W. B.; Green, M. L. H.; Jacobsen, A. J. *J. Chem. Soc., Chem. Commun.* **1976**, 781.
(4) Gamble, F. R.; Thompson, A. H. *Solid State Commun.* **1978**, *27*, 379.
(5) Clement, R.; Davies, W. B.; Ford, K. A.; Green, M. L. H.; Jacobson, J. *Inorg. Chem.* **1978**, *17*, 2754.
(6) Heyes, S. J.; Clayden, N. J.; Dobsom, C. M.; Green, M. L. H.; Wisemen, P. J. *J. Chem. Soc., Chem. Commun.* **1987**, 1560.
(7) Cleary, D. A.; Baer, D. R. *Chem. Mater.* **1992**, *4*, 112.
(8) Wong, H. V.; Millett, R.; Evans, J. S. O.; Barlow, S.; O'Hare, D. *Chem. Mater.* **1995**, *7*, 210.
(9) O'Hare, D. *Chem. Soc. Rev.* **1992**, 121 and references therein.
(10) Mathey, Y.; Clement, R.; Sourisseau, C.; Lucazeau, G. *Inorg. Chem.* **1980**, *19*, 2773.
(11) Kim, K.; Liddle, D. J.; Cleary, D. A. *J. Phys. Chem.* **1990**, *94*, 3205.
(12) Wiegers, G. A.; Meerschaut, A. Sandwiched Inconmmensurated Layered Compounds. In *Non-conmmensurated Layered Compounds*; Meerschaut, A., Eds.; Trans. Tech. Pub. Ltd.: Zurich, 1992, and references therein.
(13) Meerschaut, A.; Guemas, L.; Auriel, C.; Rouxel, J. *Eur. J. Solid State Inorg. Chem.* **1990**, *27*, 557.
(14) Meerschaut, A.; Auriel, C.; Rouxel, J. *J. Alloys Compounds* **1992**, *183*, 129.
(15) Auriel, C.; Meerschaut, A.; Roesky, R.; Rouxel, J. *Eur. J. Solid State Inorg. Chem.* **1992**, *29*, 557.
(16) Auriel, C.; Meerschaut, A.; Deniard, P.; Rouxel, J. *C. R. Acad. Sci. Paris* **1991**, *313 Ser. II*, 1255.
(17) Hernán, L.; Lavela, P.; Morales, J.; Pattanayak, J.; Tirado, J. L. *Mater. Res. Bull.* **1991**, *26*, 1211.
(18) Barriga, C.; Lavela, P.; Morales, J.; Pattanayak, J.; Tirado, J. L. *Chem. Mater.* **1992**, *4*, 1021.
(19) Hernán, L.; Morales, J.; Sánchez, L.; Tirado, J. L. *Chem. Mater.* **1993**, *5*, 1167.
(20) Oosawa, Y.; Gotoh, Y.; Akimoto, J.; Tsunoda, T.; Sohma, M.; Hayakawa, H.; Onoda, M. *Solid State Ionics* **1994**, *67*, 287.
(21) Hernán, L.; Morales, J.; Sánchez, L.; Tirado, J. L. *J. Chem. Soc., Chem. Commun.* **1994**, 1167.

0897-4756/95/2807-1576$09.00/0

reaction of cobaltocene solutions in acetonitrile with $(PbSe)_{1.12}(NbSe_2)_2$ misfit layer compound. In the present paper we extend this reaction to other misfit layer compounds of titanium and tantalum and the electronic structure of the intercalated materials is investigated by using X-ray photoelectron spectroscopy, a technique which has been demonstrated useful to describe the electronic changes by cobaltocene intercalation into $SnS_{2-x}Se_x$ ($0 \leq x \leq 2$) crystals.[22,23] The results are compared with those of the TiS_2, TaS_2, and $NbSe_2$ intercalates to shed light on the role played by the MX sublattice in these ternary chalcogenides.

Experimental Section

Polycrystalline samples of $(PbS)_{1.18}(TiS_2)_2$,[14] "$PbTa_2S_5$", and $(PbSe)_{1.12}(NbSe_2)_2$[15] were prepared by heating mixtures of the corresponding elements (supplied by Strem Chem.) in proper amounts in evacuated silica tubes. First, mixtures were heated for 1 day at 400 °C and then heated for 7 days at 900 °C. In both steps a heating rate of 1 °C/min was used. The materials were obtained as high-purity platelike crystals with a metal luster. The tubes were opened in a drybox (M Braun *250*) and the crystals were manually ground in an agate mortar.

TiS_2, TaS_2, and $NbSe_2$ were also used as host materials for comparative purposes. TiS_2 and TaS_2 were supplied by Strem Chem. and were used as received. $NbSe_2$ was obtained by direct synthesis from the elements at 900 °C. Their X-ray diffraction patterns agreed well with 1T-TiS_2, 2H-TaS_2, and 2H-$NbSe_2$ polymorphs, respectively.

Inside the glovebox, the crystalline hosts were added to a solution of $CoCp_2$, in dry acetonitrile, supplied by Strem Chem. The host/$CoCp_2$ molar ratio used was 1/1.5. The reaction was carried out at 90 °C in sealed Pyrex tubes, previously frozen under liquid nitrogen and evacuated to $P < 10^{-3}$ mbar. A heating period of a week was long enough to obtain a 100% of conversion degree. Absence of the (00*l*) reflections of the host was considered an evidence for complete intercalation. At the end of the reaction, the tube was opened in the drybox, the suspension was filtered and the solid was washed with acetonitrile. After intercalation, the particles swelled and lost the metallic luster. Then, the intercalated compounds were stored under N_2 in sealed glass tubes until their characterization. The amount of intercalated cobalt was measured by atomic absorption spectroscopy, and the stoichiometry confirmed by elemental analysis.

Powder X-ray diffraction spectra (XRD) were recorded in a Siemens D500 powder diffractometer by using monochromatized Cu Kα radiation controlled by a Siemens microcomputer. Electron diffraction patterns were obtained in a JEOL 200CX apparatus.

XPS spectra were recorded with an ESCALAB 210 spectrometer working in the constant pass energy mode (50 eV) and unmonochromatized Mg Kα (1253.6 eV) and Al Kα (1486.6 eV) radiations as excitation sources. The pressure in the analysis chamber was always below 10^{-9} mbar. The samples, as pellet made by compressing the powdered compounds at about 3 tons under an argon atmosphere, were rapidly sticked on a copper holder with a low vapor pressure epoxy resin (Torr Seal from Varian) and immediately transferred to the preparation chamber of the spectrometer ($P \leq 10^{-7}$ mbar). Prior to the analysis, the samples were scraped with a corundum file for several minutes to remove the surface contamination and to expose clean fresh surfaces. Because of the epoxy resin layer, all samples showed charging effects of 2–3 eV. The binding energy reference was taken at 161.7 eV for the S 2p core level or at 54.5 eV for the Se 3d core level, since these elements are common in the studied compounds. These binding energy values are in good agreement with those previously reported for S^{2-} and Se^{2-} species,[24] and after this calibration, the small C 1s signal arising from adventitious contamination appeared at 284.6 ± 0.2 eV BE. In some cases, Co 2p signals were analysed, after Shirley background subtraction,[25] by fitting in Lorentzian–Gaussian curves, to obtain the percentage of the different cobalt species in the samples.

In addition to the samples intercalated with cobaltocene by immersion in acetonitrile solutions, samples with cobaltocene deposited (adsorbed and intercalated) on their surface from the gas phase were also studied. These experiments were carried out in the preparation chamber of the XPS spectrometer, by dosing $CoCp_2$ vapors ($P = 4 \times 10^{-5}$ mbar) over fresh surfaces of host compounds at room temperature. This study was done to make clear the origin and nature of the two oxidized cobalt species that we found in intercalated samples in acetonitrile.

Table 1. Lattice Constants of Misfit Layered Chalcogenides

chalcogenides	subcell	*a* (Å)	*b* (Å)	*c* (Å)	β (deg)
$(PbS)_{1.14}(TaS_2)_2$	PbS	5.820(1)	5.771(2)	18.00(2)	
	TaS_2	3.303(3)	5.778(4)	17.99(3)	
$(PbS)_{1.18}(TiS_2)_2$	PbS	5.755(9)	5.869(6)	17.35(5)	93.74
	TiS_2	3.404(8)	5.869(5)	17.45(2)	93.60
$(PbSe)_{1.12}(NbSe_2)_2$	PbSe	6.142(3)	6.009(3)	37.47(2)	93.08
	$NbSe_2$	3.432(1)	5.997(2)	37.50(1)	93.06

Table 2. Cobaltocene Content (χ: Cobalt/Transition-Metal Atom Ratio), Lattice Expansion per TX_2–TX_2 Unit, and Particle Size of Pristine Chalcogenides[a]

chalcogenide	χ	Δ*c* (Å)	P.S. (μm)
TiS_2	0.20 (0.20)	5.43 (5.55)	5–10
TaS_2	0.22 (0.23)	5.49 (5.47)	10–20
$NbSe_2$	0.18 (0.31)	5.61 (5.53)	100–120
$(PbS)_{1.18}(TiS_2)_2$	0.15	5.52	50–60
$(PbS)_{1.14}(TaS_2)_2$	0.16	5.51	10–20
$(PbSe)_{1.12}(NbSe_2)_2$	0.15	5.59	10–20

[a] Values in parentheses have been taken from Dines.[1]

Results and Discussion

The X-ray diffraction patterns of $(PbS)_{1.18}(TiS_2)_2$ and $(PbSe)_{1.12}(NbSe_2)_2$ were indexed in a monoclinic symmetry. The unit cell constants are given in Table 1 and are in good agreement with X-ray single-crystal data recently reported.[14,15] Hitherto, no X-ray single-crystal structure of "$PbTa_2S_5$" had been reported. With the aid of the electron diffraction patterns, the XRD pattern was indexed on an orthorrhombic symmetry, like $(PbS)_{1.14}(NbS_2)_2$.[13] The unit cell dimensions of both sublattices are given in Table 1. The value of the *c* axis was in good agreement with the periodic length obtained by Gotoh et al.,[26] the only structural parameter reported so far. This value defines a repetitive unit consisting of two consecutive $|TaS_2|$ slabs and a |PbS| slab stacked along the *c* direction. From the $2a_{TaS_2}/a_{PbS}$ ratio a stoichiometry $(PbS)_{1.14}(TaS_2)_2$ was deduced.

The cobalt content of the intercalates together with lattice expansion produced and the average particle size of pristine samples obtained from scanning electron microscopy images are shown in Table 2. For comparison, the same parameters of the binary chalcogenide intecalates have been also included. The stoichiom-

(22) O'Hare, D.; Jaegermann, W.; Williamson, D. L.; Ohuchi, F. S.; Parkinson, B. A. *Inorg. Chem.* **1988**, *27*, 1537.
(23) Formstone, C. A.; FitzGerald, E. T.; Cox, P. A.; O'Hare, D. *Inorg. Chem.* **1990**, *29*, 3860.
(24) Wagner, C. D.; Riggs, W. M.; Davis, L. E.; Moulder, J. E.; Muilenberg, G. E. *Handbook of X-ray Photoelectron Spectroscopy*; Perkin-Elmer, Physical Electronics Division Ed., 1978.
(25) Shirley, D. A. *Phys. Rev.* **1972**, *B5*, 4709.
(26) Gotoh, Y.; Akimoto, J.; Sakurai, M.; Kiyozumi, Y.; Suzuki, K.; Oosawa, Y. *Chem. Lett.* **1990**, 2057.

Table 3. Lattice Constants of the Misfit Layer Chalcogenides Intercalated with Cobaltocene[a]

compd	subcell	a (Å)	b (Å)	c (Å)	β (deg)
$(CoCp_2)_{0.32}(PbS)_{1.14}$-	PbS	5.821(2)	5.759(4)	23.45(2)	
$(TaS_2)_2$	TaS_2	3.287(3)	5.767(2)	23.41(1)	
$(CoCp_2)_{0.31}(PbSe)_{1.12}$-	PbSe	6.198(4)	5.908(4)	48.52(2)	93.08
$(NbSe_2)_2$	$NbSe_2$	3.423(4)	6.014(5)	48.52(3)	93.06

[a] $(CoCp_2)_{0.31}(PbS)_{1.18}(TiS_2)_2$ periodic length: 22.90 Å.

etries of Ti and Ta binary sulfide adducts are in good agreement with those reported by Dines.[1] In the case of $NbSe_2$, the cobaltocene content is about 30% lower. The smaller reactivity of this compound toward the metallocene is probably related with its larger particle size. From geometrical considerations and taking into account the size of the cobaltocene molecule and the vacancies of host lattices, a value of 0.25 for the guest/host ratio is predicted.

The cobaltocene content per transition metal atom measured in ternary chalcogenides is lower than that found in binary chalcogenides. Differences in reactivity can not be due to particle size. Other effects such as the influence of MX sublattice on the TX_2 subsystem could play an important role. Moreover, on the basis of cobalt content and average particle size, the Ti compound is the ternary chalcogenide with better intercalation properties. Similar results have been obtained with other guest species such as alkali metals,[27] and they will be discussed below.

XRD patterns of ternary intercalates were indexed like those of the parent compounds. Unit cell parameters of both sublattices are included in Table 3. Unfortunately, XRD pattern of the Ti intercalate showed only peaks associated to $(00l)$ reflections as a consequence of a strong preferred orientation of the particles, even though the spectrum was recorded by sprinkling the powder on silicone grease. For this reason, we could not calculate the unit cell constants and only the periodic length was computed. Significantly, the a and b axes hardly changed upon intercalation. In contrast, a significant expansion along the c axis direction was observed. This lattice expansion is shown in Table 2 and was similar for the three ternary chalcogenides, about 5.5 Å per $MX-TX_2-TX_2$ unit packing. This value agrees also with that observed in the binary chalcogenides and suggests that, from a geometrical point of view, the MX sublattice for this guest species induces an apparently limited effect. Moreover, the values of interlayer expansion were similar to those recently reported for metal dichalcogenides single crystals[28] and are somewhat smaller than the true van der Waals dimensions of the metallocene molecule which is essentially spherical (6.98 Å × 6.76 Å). The discrepancy between the interlayer expansion and the van der Waals dimensions of cobaltocene can be ascribed either to the decrease in size of the guest molecule as a result of the ionization process undergone upon intercalation (see below) or to some interpenetration of the C–H bonds of the carbocyclic rings into the dichalcogenide layers.[28]

Other interesting finding is the absence of reaction of misfit layer sulfides belonging to "MTS_3" family (characterized by a stacking sequence $MS-TS_2-MS$[12]) with cobaltocene, under the same above experimental conditions. This behavior suggests that the cobaltocene molecule is located uniquely in the TX_2-TX_2 interlayers, whereas the $MX-TX_2$ interlayers remained empty.

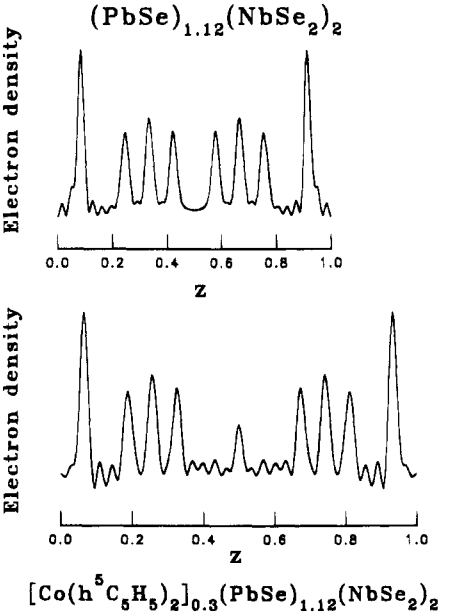

Figure 1. One-dimensional projection of the electron density along a single periodic length ($c/2$) for $(PbSe)_{1.12}(NbSe_2)_2$ and $(CoCp_2)_{0.31}(PbSe)_{1.12}(NbSe_2)_2$.

One-dimensional Patterson diagrams were used to evaluate interatomic distances along [001] in the structure of the misfit layer compounds and the products of cobaltocene intercalation. These diagrams were constructed from the integrated intensity of 13–15 multiple-order reflections (I_{l0}). The intensities were converted into experimental F_l^2 values by correction of background and Lorentz and polarization factors. The following Fourier transform was then applied:

$$P(u) = (1/c)\sum_l F_l^2 \cos(2\pi l u) \qquad (1)$$

From the u values in which maxima of the Patterson function were detected, the z coordinates of the different atoms was calculated and a set of phased structure factor F_l was generated. These were then used to obtain calculated values of I_{lc} which were compared with the experimental values by computing the R Bragg factor:

$$R_B = \sum |I_{l0} - I_{lc}| / \sum I_{l0}$$

After optimization of the z values, the one-dimensional electron density function was then computed along the z axis of the structure, according to the following expression:

$$\varrho(Z) = (1/c)\sum_l F_l \cos(2\pi l z) \qquad (2)$$

The one-dimensional electron density function of $(PbSe)_{1.12}(NbSe_2)_2$ and the product of cobaltocene intercalation are plotted against z in Figure 1. This plot reveals the expected sequence of atoms along [001] in the pristine solid: (Se,Pb)–Se–Nb–Se–Se–Nb–Se–(Se,Pb), since the PbSe subcell viewed along [001] has Se and Pb atoms slightly different from coplanarity at each side of the bilayer subunit. Similarly, after cobal-

(27) Lavela, P.; Morales, J.; Tirado, J. L. *J. Mater. Chem.* **1994**, *4*, 1413.

(28) Wong, H. V.; Evans, J. S. O.; Barlow, S.; Mason, S. J.; O'Hare, D. *Inorg. Chem.* **1994**, *33*, 5515.

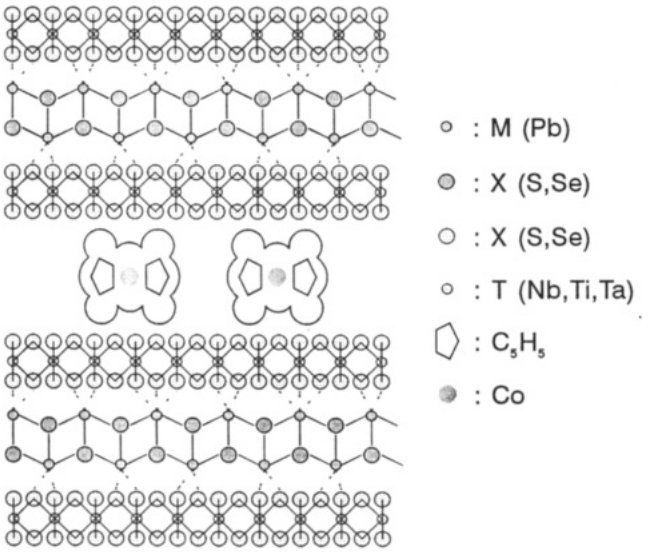

Figure 2. Schematic projection along [100] for intercalated compounds $(CoCp_2)_x(MT)_{1+y}(TX_2)_2$.

tocene intercalation the units (Se,Pb)−Se−Nb−Se and Se−Nb−Se−(Se,Pb) remained basically unaltered while the observed expansion affected almost exclusively the Se−Se distances between successive $NbSe_2$ layers, i.e., the only true van der Waals gap in this structure. Moreover, the position of cobalt atoms in the structure is evident at $z = 0.5$. This allow us to rule out the existence of possible multilayers of cobaltocene molecules parallel to the layers, as found in the intercalation of (2-aminoethyl)ferrocene in MoO_3.[29] Concerning the relative orientation of the layers and inserted molecules, it should be noted that due to the low scattering factor of carbon atoms, as compared with other atoms in the composition of the studied samples, a precise location of these atoms cannot be established. Nevertheless, if the cyclopentadienyl groups had the C_5 axis normal to the layers, a single effect should be expected from the phase contribution of the five carbon atoms. In contrast, if the cyclopentadienyl rings are allowed to have their C_5 axis parallel to the layers, each carbon atom is located at different places along the [001] direction. A model based on the free rotation of the cobaltocene molecule around Co atoms could also be indistinguishable.

Although there is some controversy concerning the metallocene orientation within the van der Waals gap of metal dichalcogenides, recent results of solid-state ^2H NMR spectroscopy and neutron diffraction[28] show that for the intercalates of ZrS_2 and $SnSe_2$ with cobaltocene, the organometallic molecule adopts an orientation in which the C_5 molecular axis lies parallel to the host layers. Such orientation should be the most suitable for the fitting of the one-dimensional electron density projections. A model proposed for the intercalates is shown in Figure 2.

Electron diffraction patterns recorded with the incident beam parallel to [001] direction were coincidental for both the pristine and intercalate compounds (Figure 3). These electron diffraction patterns are characterized by two sets of spots corresponding to the two sublattices associated with the MX and TX_2 slabs. These two

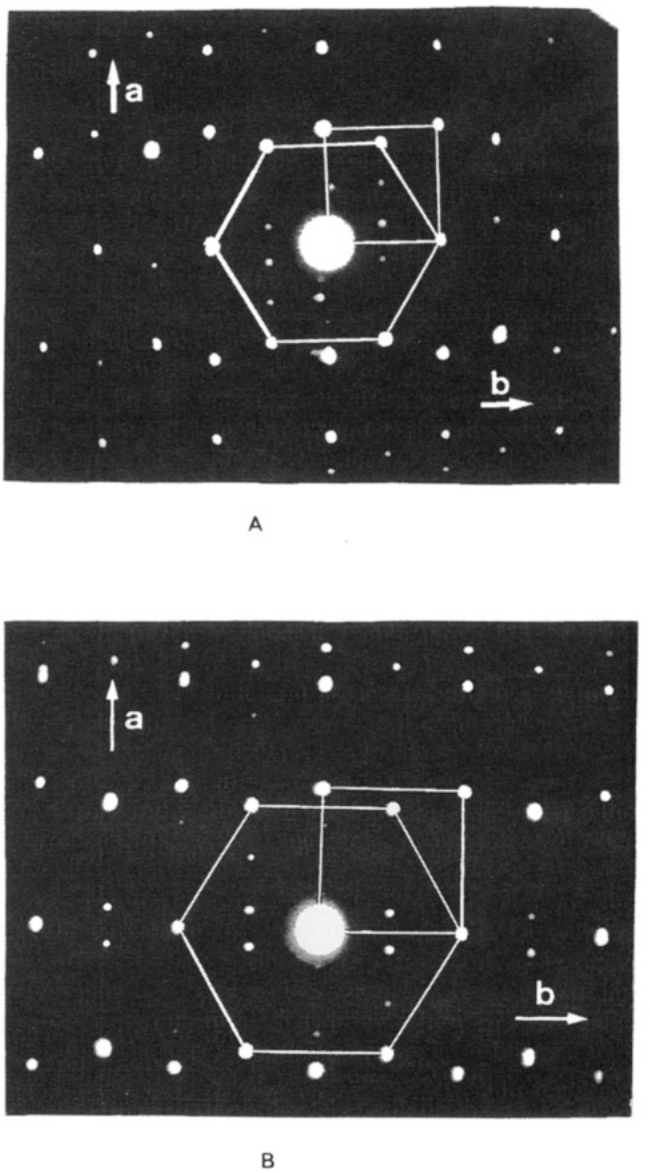

Figure 3. Experimental [001] zone electron diffraction patterns of (A) $(PbSe)_{1.12}(NbSe_2)_2$ and (B) $(CoCp_2)_{0.31}(PbSe)_{1.12}(NbSe_2)_2$.

subcells have a b^* axis of equal length, but they have a different periodicity and show an irrational ratio in the direction of the a^* axis, consistent with the incommensurate character of both sublattices. The electron diffraction patterns of the intercalate phases are very similar as a consequence of the topotactic nature of the process. The observation of a single relative orientation of both sublattices can be considered as an indirect proof that cobaltocene intercalation takes place between consecutive TX_2 slabs. In fact, it has been shown that alkali metal intercalation into $(MS)_{1+y}TS_2$ (M = Sn, Pb; T = Ti, Nb, Ta) slabs leads to orientation anomalies between both sublattices.[30] The electron diffraction patterns also confirm the X-ray diffraction results concerning the unchanging misfit between sublattices, as shown by the constancy of the a_{TX_2}/a_{MX} ratio.

Finally, the poor cobaltocene intercalation properties of the sulfide sample, $(PbS)_{1.14}(NbS_2)_2$, as compared with $(PbSe)_{1.12}(NbSe_2)_2$ were also clear from X-ray and elec-

(29) Chatakondu, K.; Formstone, C.; Green, M. L. H.; O'Hare, D.; Twyman, J. M.; Wiseman, P. J. *J. Mater. Chem.* **1991**, *1*, 205.

(30) Hernán, L.; Morales, J.; Pattanayak, J.; Tirado, J. L. *J. Solid State Chem.* **1992**, *100*, 262.

Table 4. Binding Energies and Full Widths at Half-Maximum of the Main Core Level Spectra in Pure Chalcogenides

	S 2p or Se 3d		Pb $4f_{7/2}$		Ti $2p_{3/2}$ Ta $4d_{3/2}$[a] Nb $3d_{3/2}$		
	B.E.	fwhm	B.E.	fwhm	B.E.	fwhm	B.E.
TiS_2	161.7	2.6			457.1	2.0	0.0
TaS_2	161.7	2.6			239.7	5.2	0.0
$NbSe_2$	54.6	2.1			204.4	1.5	0.0
$(PbS)_{1.18}(TiS_2)_2$	161.7	2.5	138.3	1.6	457.1	2.3	0.6
$(PbS)_{1.14}(TaS_2)_2$	161.7	2.5	138.1	1.6	239.7	4.7	0.0
$(PbSe)_{1.12}(NbSe_2)_2$	54.6	2.1	138.3	1.6	204.5	1.5	0.0
PbS	161.7	2.3	138.4	1.5			0.0

[a] Ta $4d_{5/2}$ peak, at B.E. = 227.0 overlaps with S 2s at B.E. = 226.1 eV.

tron diffraction data and agree with previous results obtained for 2H−NbS_2 and 2H−$NbSe_2$. While cobaltocene intercalation into 2H−$NbSe_2$ was reported by Dines,[1] Clement et al.[5] were unable to obtain intercalation products by direct reaction of different metallocenes with 2H−NbS_2. This is probably due to the high degree of intercalated niobium in the crystals prepared at high temperature, thus preventing intercalation.[31] In this context, Auriel et al.[32] have recently shown that the octahedral holes defined between the close-stacked NbS_2 slabs in $(PbS)_{1+y}(NbS_2)_2$ are partly filled with additional Nb atoms.

For a deeper understanding of the guest−host interaction, we have investigated the electronic structure by XPS carefully studying the core levels of layered compounds and their intercalates. Thus, for the nonintercalated ternary and binary chalcogenides, S_{2p} and Se_{3d} spectra consist of a single peak each (the spin−orbit components are unresolved due to the low resolution of the spectrometer), and they lack features (shoulders, shape or width changes; see Table 4), indicative of the presence of several chemical environments of these two elements. This suggests that the electron population of the chalcogen atom, S or Se, is similar in both binary and ternary chalcogenides and, therefore, similar in both sublattices within the ternary compounds. It also explains that these core levels have been used as references for the binding energy scale of the XPS spectra, a choice which is also supported by the constancy of the binding energy of the valence band maximum (VBM), equal to zero for most of the studied samples in this work.

A similar result is also obtained from the comparison of the binding energies of the main metallic core levels (Nb 3d, Ta 4d, Ti 2p, and Pb 4f) for the ternary chalcogenides to those for the binary ones, as shown in Table 4. Moreover, these binding energy values are very similar to those obtained for other related chalcogenides—$(PbS)_{1.14}NbS_2$, $(PbS)_{1.13}TaS_2$, $(SnS)_{1.20}$ TiS_2, SnS, PbS, NbS_2, TiS_2, and TaS_2—by other authors,[33,34] once the differences of the origin of the energy scale have been taken into account. In summary, the binding energies of all the elements (metal and chalcogen) in the misfit layer compounds do not shift with respect to the value for the pure binary chalcogenides, a fact that indicates clearly that the chemical bonding within the two different constituent layers in these compounds seems to remain invariant as compared with that of binary ones. In other words, no significant charge transfer takes place from the MX layers to the TX_2 slabs, in good agreement with previous data by X-ray photoemission.[34]

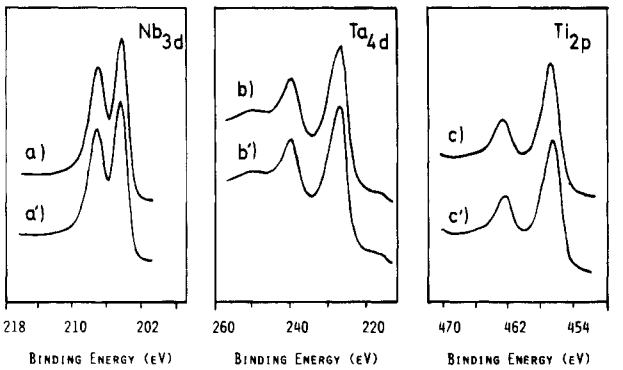

Figure 4. Ti 2p, Nb 3d, and Ta 4d core level spectra for pure and cobaltocene (G = $CoCp_2$) intercalated ternary chalcogenides: (a) $(PbSe)_{1.12}(NbSe_2)_2$, (a′) $G_{0.31}(PbSe)_{1.12}(NbSe_2)_2$; (b) $(PbS)_{1.14}(TaS_2)_2$, (b′) $G_{0.32}(PbS)_{1.14}(TaS_2)_2$); (c) $(PbS)_{1.18}(TiS_2)_2$; (c′) $G_{0.31}(PbS)_{1.18}(TiS_2)_2$.

The intercalation of cobaltocene in the binary and ternary chalcogenides studied in this work, by immersion in acetonitrile solutions or by dosing in situ with cobaltocene vapor, does not change significantly either the binding energy, shape, or width of any core emission peaks of the substrates, as shown in Table 5 for all the studied compounds. In particular, this constancy is noteworthy in the case of core-level emission peaks of the Ti, Nb, and Ta, depicted in Figure 4, given that these atoms are susceptible to be chemically reduced by cobaltocene according to the reaction

$$x\mathrm{CoCp_2} + (\mathrm{PbX})_{1+y}(\mathrm{TX_2})_2 \rightarrow (\mathrm{CoCp_2})_x^{+}[(\mathrm{PbX})_{1+y}(\mathrm{TX_2})_2]^{x-} \quad (3)$$

The behavior of these transition-metal chalcogenides differs from that found in the series $SnS_{2-x}Se_x$ ($0 \le x \le 2$).[23] In this case, as a consequence of cobaltocene intercalation, the XPS spectra revealed the splitting of the Sn 4d emission peak, which resulted in the appearance of a shoulder at lower binding energy than that of the main peak for all the members of the series. This has been explained in terms of mixed oxidation states for tin, Sn(II) and Sn(IV), an observation which has been taken as evidence for an electron transfer between the guest and host upon intercalation.

On the other hand, the evolution of the Co 2p and C 1s spectra as a function of the cobaltocene content is presented in Figure 5 for the case of $(PbSe)_{1.12}(NbSe_2)_2$ as an illustration of the general behavior of these intercalates. Thus, in the course of $CoCp_2$ deposition, a main Co 2p doublet is growing in at BE(Co 2p3/2) = 782.6 ± 0.2 and BE(Co 2p1/2) = 797.5 ± 0.4 eV, with small differences in BE and/or fwhm among substrates (see Table 5 and Figure 5), together with a growing C 1s signal at BE = 286.0 ± 0.1 eV due to the carbon atoms in the cyclopentadienyl ring. As can be seen in Figure 5, the main Co 2p doublet is also accompanied

(31) Whittingham, M. S.; Gamble, F. R. *Mater. Res. Bull.* **1975**, *10*, 363.
(32) Auriel, C.; Meerschaut, A.; Rouxel, J. *Mater. Res. Bull.* **1993**, *33*, 675.
(33) Ohno, Y. *Phys. Rev. B* **1991**, *44*, 1281.
(34) Ettema, A. R. H. F.; Haas, C. *J. Phys. C: Condens. Matter* **1993**, *5*, 3817.

Table 5. Binding Energies and Full Widths at Half-Maximum of the Main Core Level Spectra in $CoCp_2$ Intercalated Chalcogenides

	S 2p Se 3d		Pb $4f_{7/2}$		Ti $2p_{3/2}$ Ta $4d_{3/2}$[a] Nb $3d_{3/2}$		Co $2p_{3/2}$[b]		C 1s	
substrate	B.E.	fwhm	B.E.	fwhm	B.E.	fwhm	B.E.	fwhm	B.E.	fwhm
TiS_2	161.7	2.7			457.1	2.0	782.5	1.9	286.0	2.0
TaS_2	161.7	2.6			239.7	5.2	782.5	1.9	286.0	2.2
$NbSe_2$	54.6	2.2			204.4	1.5	782.6	2.0	286.3	2.0
$(PbS)_{1.18}(TiS_3)_2$	161.7	2.4	138.3	1.6	457.1	2.3	782.6	1.8	286.1	2.1
$(PbS)_{1.14}(TaS_2)_2$	161.7	2.5	138.1	1.6	239.7	4.7	782.4	2.0	285.9	2.2
$(PbSe)_{1.12}(NbSe_2)_2$	54.6	2.1	138.3	1.6	204.5	1.5	782.4	2.1	286.0	2.0

[a] Ta $4d_{5/2}$ peak, at B.E. = 227.0 overlaps with S 2s at B.E. = 226.1 eV. [b] Co $2p_{3/2}$ main peak.

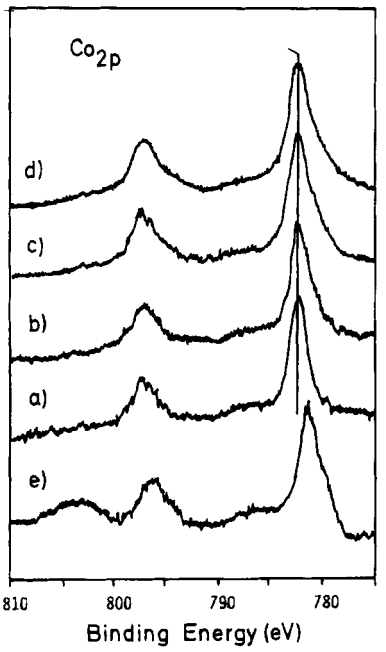

Figure 5. Co2p core level spectra in the course of $CoCp_2$ deposition for $(PbSe)_{1.12}(NbSe_2)_2$: (a) 1200 L; (b) 3600 L; (c) 45000 L. (d) Intercalate prepared in solution. (e) Co 2p core level spectrum of $CoCp_2$ adsorbed on Cu.

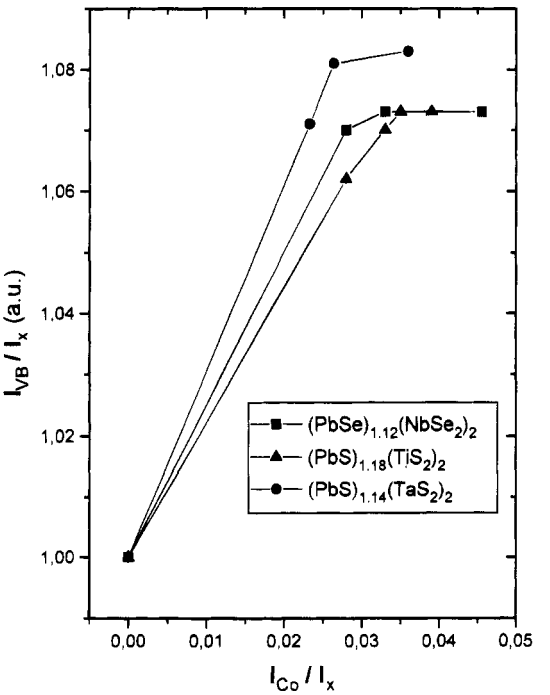

Figure 6. Evolution of the VB intensity as cobaltocene content for ternary chalcogenides. (X = S, Se.)

by the appearance of tails at the low binding energy side of the main peaks for high cobaltocene contents (ex situ intercalates and long $CoCp_2$ deposition times) that accounts for the presence of a second cobalt species. The intensity of this minor species depends on the particular substrate and increases with the cobaltocene concentration, the maximum values being reached for samples intercalated in acetonitrile. By fitting of the Co 2p spectra, the percentage of this minority species has been estimated to be 20 ± 3% of the total cobalt content for the different substrates.

In contrast, cobaltocene adsorbed on a clean surface (Ar^+ sputtered) of the Cu sample holder produces a single Co 2p spectrum—also shown in Figure 5—located at BE(Co 2p3/2) = 781.3 eV. In this case, the binding energy was measured with respect to the Cu 2p3/2 line at 932.7 eV.

The high BE value of the main Co 2p photoemission peaks found for intercalate samples and the very low intensity of the shake-up satellite signal at BE ~ 788 eV suggest that they are due to Co^{3+} species.[7,23,35] On the other hand, the spectrum found by adsorption of $CoCp_2$ on Cu, with lower BE and higher shakeup satellites agrees with the presence of Co^{2+} species.[22]

Concerning the valence band region, only a small increase in the intensity of the global emission is observed by XPS as the amount of cobaltocene (adsorbed or intercalated) increases, as shown in Figure 6. This rise, which is found for all the intercalates, mainly occurs during the first deposition steps, and a saturation level is very soon reached. Unfortunately, the energy resolution of our conventional XPS spectrometer is not high enough to separate the several components in the valence band, so that it is no possible to know which orbitals—from the transition metal or the chalcogen atoms—have been filled. In any case, it seems that deposition of $CoCp_2$ induces an increase in the electron population of the valence band, which suggests a charge transfer from the adsorbate molecules to the substrate. In this sense, the saturation level in the VB intensity is always found before reaching the saturation in cobaltocene deposition, as shown in Figure 6. Thus, part of the cobaltocene molecules will remain unoxidized, in good agreement with a second species of cobalt observed in the XPS spectra.

These results seem to indicate that the first gas molecules of $CoCp_2$ reacting with the substrate matrix,

(35) van Elp, J.; Wieland, J. L.; Eskes, H.; Kuiper, P.; Sawatzky, G. A.; de Groot, F. M. F.; Turner, T. S. *Phys. Rev. B* **1991**, *44*, 6090.

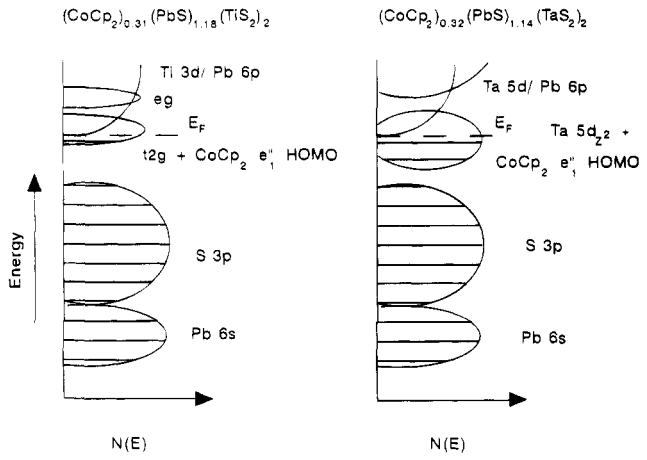

Figure 7. Schematic band structure diagrams for misfit layer compounds intercalated with cobaltocene.

which are likely intercalated into the van der Waals layers defined at the TX_2/TX_2 interfaces, undergo a rapid oxidation process to $CoCp_2^+$, while electrons are transferred to the valence band of the chalcogenide. As the film thickness of $CoCp_2$ increases, the charge electron transfer from the organometallic molecule to the host becomes more difficult and the intensity of the low-energy peak, assigned to unoxidized $CoCp_2$ molecules, increases.

For a better understanding of the process of electron transfer between the guest and the host, a knowledge of the band structure of misfit layer compound is required. According to photoelectron studies, the band structure of misfit layer compounds is a superposition of the band structure of the component sublattices.[36] The density of states as a function of energy is shown in Figure 7 for two representative cases. The transition metal d bands lie above the sulfur valence band. The splitting of the d band depends on the ligand field symmetry. Thus, the octahedral symmetry splits the d orbitals into a lower t_{2g} and a higher e_g band. This is the case for titanium compounds that in principle have the t_{2g} band unoccupied, except that some charge transfer from the MS layer to the TiS_2 occurs as in $(PbS)_{1.18}TiS_2$, for which the number of conduction electrons is about 0.4/Ti atom,[37] and the compound behaves as a metallic conductor. In trigonal prismatic coordination, the t_{2g} band splits into two new bands, a doublet e′ of higher energy (d_{xy}, $d_{x^2-y^2}$) and a lower singlet a_1 formed by the d_{z^2} orbital. This occurs in Nb and Ta misfit layer compounds and for these elements the d_{z^2} band is half-filled (see Figure 7).

In agreement with this model the donor levels of $CoCp_2$, in particular its highest occupied molecular orbitals e''_1, are adjacent to the acceptor transition-metal sites. Electron transfer would take place by overlapping of the lowest unoccupied d-band levels with the antibonding e''_1 orbitals of cobaltocene. This simple picture accounts for the better intercalation properties of Ti misfit layer sulfide, reflected in the stoichiometry values listed in Table 2, that may accommodate in the broad t_{2g} band up to six electrons per transition metal atom.

In contrast, for $(PbX)_{1+y}(TX_2)_2$ misfit compounds with T = Nb or Ta, the low-energy a_1 level is already occupied, formally half-filled with the d electrons of the transition metal. This occupancy would make difficult the electron transfer promoted by the cobaltocene intercalation and, hence, would explain the worse intercalation properties of these ternary compounds.

Two main conclusions can be drawn from the XPS results. First, clear evidence has been found for the oxidation of $CoCp_2$ to $CoCp_2^+$ upon intercalation. This observation has been taken as a proof that an electron transfer occurs between the guest molecule and the host framework. However, such a process does not affect appreciably the binding energies of the core electrons of the host constituent elements, in particular the transition element, which are sensitive to undergoing a reduction process. This agrees with that generally observed in the early transition-metal dichalcogenides, whose core level binding energies do not undergo large changes upon intercalation of different guest species. This has been explained on the basis of the high density of states near the Fermi level that can accommodate a significant number of electrons, maintaining basically the same electronic structure.[38]

The presence of a Co^{2+} species has also been detected. From magnetic measurements, small quantities of this cobalt oxidation state has been found in $(CoCp_2)_{0.25}TaS_2$,[4] whose origin has been adscribed to contamination from surface adsorbed $CoCp_2$. However, such an explanation is unlikely for the intercalates studied in this paper, where probably a significant amount of unoxidized cobaltocene could remain intercalated as neutral molecule. A mixture of $CoCp_2$ and $CoCp_2^+$ has been also proposed for the intercalation compounds formed between cobaltocene and different hosts such as $SnSe_2$[22,23] and $Cd_2P_2S_6$.[11]

None of the Co $2p_{3/2}$ emission peaks of the differents intercalates studied in this paper can be resolved in three components as found in tin selenides intercalates[23] and which have been associated with three cobalt species Co(I), Co(II), and Co(III). Consequently, the present study has not allowed us to confirm the formation of a reduced cobaltocene species in the intercalation process of this metallocene into transition-metal layered chalcogenides.

Acknowledgment. This work has been financially supported by CICYT (Project MAT 93-1204) and Consejería de Educación y Ciencia (Junta de Andalucía).

CM9501426

(36) Ettema, A. R.; Haas, C.; Turner, T. S. *Phys. Rev. B* **1993**, *47*, 12794.

(37) Wiegers, G. A.; Haange, R. J. *Eur. J. Solid State Inorg. Chem.* **1991**, *t28*, 1071.

(38) Ettema, A. Ph.D. Thesis, University of Groningen, Netherlands, 1993.